RSC Advances

ROYAL SOCIETY OF CHEMISTRY

www.rsc.org/advances

Synthesis of polypyrrole nanoparticles for constructing full-polymer UV/NIR-shielding film

Xiaoliang Chen,[a] Nuo Yu,[a] Lisha Zhang,[*b] Zixiao Liu,[a] Zhaojie Wang,[a] and Zhigang Chen[*a]

Abstract: A prerequisite for the selective shielding of solar light is to develop optical materials and coatings, and traditional shielding materials usually combine rare/expensive metal elemental and also have potential heavy-metal pollution after being abandoned. To solve this problem, herein we develop polypyrrole (PPy) nanoparticles as a novel kind of metal-free ultraviolet (UV)/near-infrared (NIR) shielding material. PPy nanoparticles with diameter of ~50 nm are synthesized by a simple solution polymerization route, and they exhibit weak absorption in visible region but strong UV/NIR photoabsorption. Subsequently, PPy nanoparticles are mixed with polyacrylic acid (PAA) resin for the preparation of PPy-PAA full-polymer films. PPy-PAA films exhibit good transparency in visible region (400-780 nm) but can efficiently absorb UV (305-400 nm) and NIR (780-2500 nm) light, for example, 0.34-mm-thick film with 0.05 wt% PPy can transmit 63.1% visible light but shield 47.2% UV and 80.9% NIR light. When this PPy-PAA film coated glass is used as the window of the sealed black box, the interior air temperature of the box goes up from room temperature of 25.0 °C to 29.2 or 33.9 °C in 1500 s under the irradiation of strong solar light (0.3 or 0.5 W cm^{-2}). Its temperature elevation (4.2 or 8.9 °C) is remarkably lower compared with that (7.3 or 15.7 °C) from glass slide as window under the other identical condition, resulting from excellent NIR shielding property of PPy. Therefore, PPy nanoparticles have great potential as

[a]*State Key Laboratory for Modification of Chemical Fibers and Polymer Materials, College of Materials Science and Engineering, Donghua University, Shanghai 201620, China. E-mail: zgchen@dhu.edu.cn*

[b]*College of Environmental Science and Engineering, Donghua University, Shanghai 201620, China. E-mail: lszhang@dhu.edu.cn*

a novel UV/NIR shielding material for the development of cost-efficient energy-saving full-polymer windows without potential heavy-metal pollution.

Keywords: polypyrrole nanoparticles; synthesis; UV/NIR; shielding film; energy-saving windows

1. Introduction

Optical materials and coatings have played a vital role in selectively shielding solar light for meeting the growing demand of thermoshygrometric and environmental comfort as well as improving the energy efficiency of buildings (or automobile).[1, 2] The most ideal optical materials and coatings should be smart glass which changes between translucent and transparent when voltage/light/heat is applied. The typical smart glass includes electrochromic (such as WO_{3-X} and NiO_X-based),[3, 4] photochromic (such as WO_3 and MoO_3-based),[5, 6] thermochromic (such as VO_2-based)[7] devices, which results in great contributions to the progress in selectively shielding solar light. However, smart glass is still immature for the large-scale practical applications in buildings and automobile. In fact, for selectively shielding solar light in most applications, it would be the most simple and affordable choice to directly use semi-transparent heat-insulation coating which can absorb/reflect part of solar light. It is well known that solar light is chiefly concentrated in the wavelength range between 0.2 and 2.5 μm, including ultraviolet (UV, 0.2~0.4 μm, 4% of total energy), visible (0.4~0.78 μm, 46% of the total energy), near infrared (NIR, 0.78~4.5 μm, ~50% of total energy) light. For

[a]State Key Laboratory for Modification of Chemical Fibers and Polymer Materials, College of Materials Science and Engineering, Donghua University, Shanghai 201620, China. E-mail: zgchen@dhu.edu.cn
[b]College of Environmental Science and Engineering, Donghua University, Shanghai 201620, China. E-mail: lszhang@dhu.edu.cn

simultaneously satisfying visual effects and reducing the heating/adverse effect, it is necessary to develop UV/NIR-shielding coating which can only transmit visible light but cut off both NIR and UV light. The use of this UV/NIR shielding coating will prevent a temperature elevation in a room in summer and realize heat-insulating in winter, and it is also desirable for health care.

Currently, the widely used photo-shielding coating should be metal (such as Ag, Cu) film,[8, 9] which can reflect part of visible and IR light. These metal films are usually prepared by vacuum thermal evaporation or magnetron sputtering, which is too costly and would hinder large-scale production. To solve this problem, the solution-process of metal-based nanomaterials and the corresponding nanomaterial-contained polymer film have been demonstrated to be a good alternative to conventional metal films. The key for this technology is to obtain efficient UV/NIR shielding nanomaterials. Three kinds of UV/NIR shielding nanomaterials have been well developed. The first one is noble metal nanoparticles, such as Ag/Au nanoparticles,[10] but it shows low visible light transparency. The second one is rare-earth hexaboride nanoparticles, but it can only absorb certain wavelengths of NIR and the preparation process need the complex high temperature (~1500 °C) and vacuum conditions.[11, 12] The last kind is metal-oxide semiconductor nanomaterials, which should be the most studied UV/NIR shielding nanomaterials. For example, both tin-doped indium oxide (ITO)[13, 14] and Al-doped zinc oxide (AZO)[15, 16] nanoparticles have been demonstrated to exhibit NIR photoabsorption ability, but they are famous transparent conductive materials and can only shield NIR light with wavelength longer than 1500 nm. To broaden NIR photoabsorption range, tungsten (W)-based nanomaterials have been well developed, including $W_{18}O_{49}$[17, 18] and M_xWO_3 (M^{x+} = Na^+ , K^+ , Rb^+ , Cs^+ and NH_4^+).[19-22] These W-based nanomaterials can

transmit visible light but shield NIR light, resulting in great contributions to the progress in shielding materials. It should be noted that all these metal-based materials involve in the utilization of expensive and/or rare metal (In, W, et al), and the abandon of the heavy-metal-contained films would deteriorate the environment, both of which would partly limit their application ranges. Therefore, it is very necessary to develop novel kind of cost-efficient UV/NIR shielding materials without metal component.

Recently, several kinds of NIR light-driven photothermal nanoagents have been well developed for biomedical applications, inducing polymer (such as polypyrrole (PPy)),[23, 24] metal (such as Au),[25, 26] carbon (such as graphene),[27] semiconductors (such as CuS).[28] Our group has developed W-based ($W_{18}O_{49}$[29, 30] and Cs_xWO_3[31]) nanomaterials, Cu-based (CuS[32], Cu_9S_5[33], Fe_3O_4@$Cu_{2-x}S$[34]) nanomaterials as efficient NIR photothermal agents. All these photothermal nanoagents exhibit very strong photoabsorption in NIR region. Compared with W-based and Cu-based nanomaterials, we also found that polypyrrole (PPy) nanoagents have very broad UV/NIR photoabsorption range and they are metal-free. These features trigger our interest in developing PPy nanomaterials as a new kind of cost-efficient UV/NIR shielding agent without potential heavy-metal pollution. In the present work, we have prepared PPy nanoparticles with diameter of ~50 nm by one-step aqueous dispersion polymerization. PPy nanoparticles exhibit high transparency in visible region (400-780 nm) but absorb efficiently UV/NIR light. With PPy nanoparticles and polyacrylic acid (PAA) resin as the mode, flexible PPy-PAA composite films are prepared by using coating/drying technology. One of typical PPy-PAA films (thickness: 0.34 mm, PPy content: 0.05 wt%) can transmit 63.1% visible light (400-780 nm) but shield 47.2% UV and 80.9% NIR light. Importantly, with this PPy-PAA film coated glass as the window of the sealed box, the interior air temperature exhibits

obviously low elevation (4.2 or 8.9 ℃) compared with that (7.3 or 15.7 ℃) from glass slide as the window, under the irradiation of solar light with high intensity (0.3 or 0.5 W cm^{-2}).

2. **Experimental details**

2.1 Materials

All of the chemicals are commercially available and were used without further purification. Iron (III) chloride hexahydrate ($FeCl_3$•$6H_2O$, 99%), polyvinyl alcohol (PVA, molecular weight ~1750), pyrrole monomer (98%) were received from Sinopharm Chemical Reagent Co., Ltd (China). Polyacrylic acid (PAA, molecular weight ~20000) resin was purchased from HanwHA Corporation.

2.2 Synthesis of PPy nanoparticles

PPy nanoparticles were synthesized by a modified one-step aqueous dispersion polymerization method.[24] $FeCl_3$•$6H_2O$ (4.6 mmol, 1.2347 g) and PVA (1.5 g) were dissolved into the deionized water (50 mL) at room temperature under magnetically stirring, forming a transparent yellow solution. After 1 hour equilibration, the solution was transferred to an ice-water bath. Subsequently, pyrrole monomer (2.0 mmol, ~140 μL) was added into the above solution. When pyrrole monomer contacted the oxidizing agent ($FeCl_3$), polymerization reaction proceeded immediately. The mixture solution became black within a few minutes and was continuously stirred for 4 hours. After the completion of polymerization, the system was boosted to room temperature naturally. The resulting sample was separated via centrifugation and was washed three times with hot water to remove impurities. Finally, the precipitation was dispersed in the deionized water with concentration of 0.5 mg mL^{-1}, and the aqueous dispersion was stored at refrigerator at 4 °C for further use.

2.3 Preparation of PPy-PAA films

In a typical film synthesis process, PAA resin (2.0 g, ~2.0 mL) was dispersed in the deionized water (2.0 mL) under magnetically stirring. Then this PAA resin dispersion was mixed with PPy aqueous dispersion (2.0 mL, 0.5 mg mL^{-1}) under stirring, forming a homogeneous dark colloidal dispersion (slurry). Subsequently, the above slurry with different volumes (1.0, 1.5, 2.0 mL) was coated on the glass slides, respectively. Then the glass slides were respectively placed on a hotplate at 50 °C to remove solvent, until PPy-PAA films were solidified. PPy-PAA full-polymer films with 0.05 wt% PPy and different thickness (~0.34, 0.50, 0.60 mm) could be easily peeled off from the glass slides. For comparison, 0.50 mm-thick PPy-PAA films with different PPy content (0.10 wt%, and 0.125 wt%) were also prepared by changing the volume (4.0 or 5.0 mL) of suspension containing PPy nanoparticles with the other identical conditions.

2.4 Characterization and NIR shielding measurements

The morphologies of PPy nanoparticles and PPy-PAA films were investigated by using a field emission-scanning electron microscopy (FE-SEM, Hitachi S-4800) and transmission electron microscopy (TEM, JEOL JEM-2100F). The Fourier transform infrared (FT-IR) spectrum was measured from PPy sample in KBr pellets using an IRPrestige-21 spectrometer (Shimadzu). UV-vis absorbance spectrum of PPy suspension was recorded on a Shimadzu UV-2550 UV-visible-NIR spectrophotometer using a quartz cuvette with an optical path of 10 mm. The thickness of PPy-PAA composite films was measured by vernier caliper. In order to measure its photothermal effect, PPy powder (0.5 mg) was put on the white paper. PPy sample was irradiated by a Xenon lamp with the intensity of 0.5 W cm^{-2}, and its temperature was real-time recorded by an infrared thermal imaging camera (FLIR A300).

To evaluate NIR shielding performance, the transmittance spectra of PPy-PAA films were measured on a UV-visible-NIR spectrophotometer from 300 to 2500 nm (Shimadzu UV-3600). To further measure the heat-insulation performance, we constructed two sealed boxes, as illustrated in Fig. 1, where glass slides or PPy-PAA film-coated glass (2×6 cm^2) was used respectively as the window. The environmental air temperature was 25 °C. An adjusted xenon lamp (PLS-SXE300/300UV, Beijing Perfect Light Co. Ltd., Beijing) was used as the simulated solar light source and the light intensity was independently calibrated using a hand-held optical power meter (Newport model 1918-C, CA, USA). For amplifying the heating effect of solar light, solar light with high intensity (0.3 or 0.5 W cm^{-2}) was used to illuminate the box through the window, and then the air-temperature in the box was real-time recorded by using an electronic thermometer that should not be directly illuminated by light.

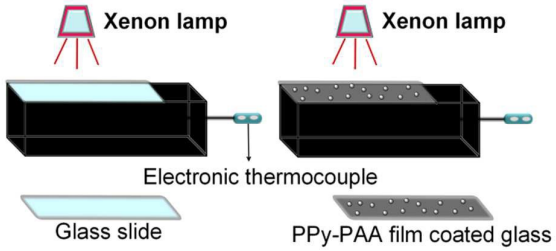

Fig. 1 Schematic illustration of the sealed black boxes, where only the top facet was covered by glass slides or PPy-PAA film coated glass.

3. Results and discussion

3.1 Preparation and characterization of PPy nanoparticles

PPy nanoparticles were synthesized by a modified one-step aqueous dispersion polymerization with PVA as the stabilizer and $FeCl_3$ as the oxidizing agent.[23] The morphology and size of PPy sample were studied by SEM images (Fig. 2a). Obviously, PPy sample consists of exclusively spheral nanoparticles with narrow particle size distribution, and the average size is about 50 nm. In addition, TEM images (Fig. 2b) further confirm the formation

of PPy nanospheres with diameter of ~50 nm.

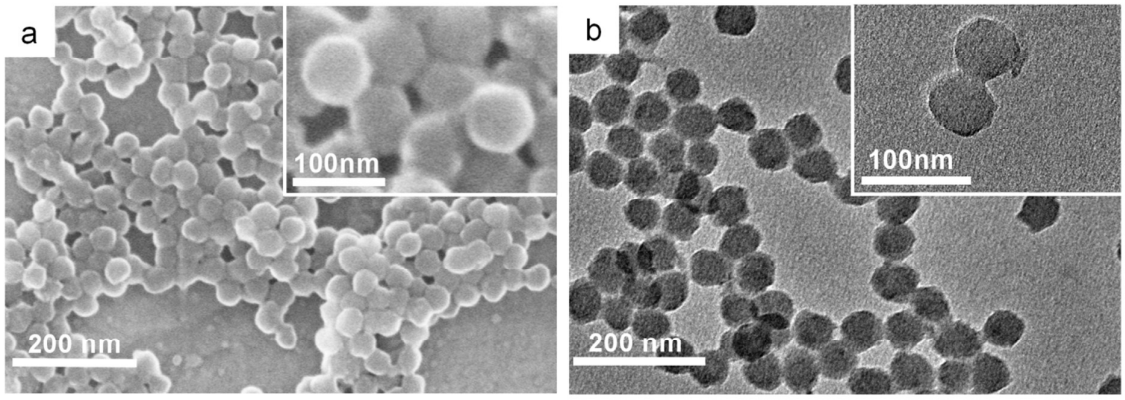

Fig. 2 SEM (a) and TEM (b) images of PPy nanoparticles.

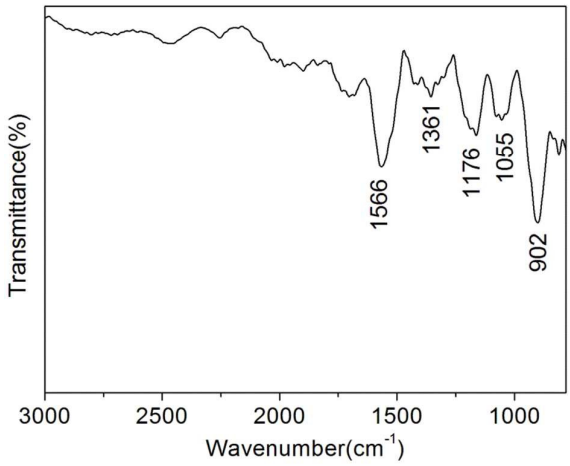

Fig. 3 FTIR spectrum of PPy nanoparticles.

Subsequently, PPy nanoparticles were identified by FTIR spectrum (Fig. 3). Obviously, PPy nanoparticle sample exhibits a band at 1566 cm^{-1}, which is assigned to the stretching vibration of C = C units.[35] The band at 1361 cm^{-1} is corresponding to the stretching vibration of C-N adsorption.[36] The bands at 1176 and 1055 cm^{-1} are attributed to the =C-N in-plane deformation vibrations. In addition, the broad band near 902 cm^{-1} is corresponds to =C-N out-plane deformation vibration.[35, 37] Based on the above results, one can confirm the formation of PPy material. [36]

The aqueous dispersion containing PPy nanoparticles (60 μg mL^{-1}) exhibits a strong

black color (the inset in Fig. 4), and has high stability, even remaining unchanged after several weeks at 4 °C. In addition, the optical property of the aqueous dispersion was studied by using UV-vis-NIR spectroscopy (Fig. 4). The spectrum is similar to that in the previous reports on PPy nanoparticles,[23, 24] and it exhibits the short-wavelength absorption edged at approximately 250 nm. Obviously, the sample has low absorbance in the visible region (400-650 nm) with the lowest absorbance of 1.21 at 570 nm, indicating the fact that part of visible light can be transmitted through PPy solution. Importantly, the spectrum shows an increased absorption with the increase of wavelength from 570 to 988 nm, where the maximum extinction coefficient at 988 nm was calculated to be 3.83×10^4 cm^2 g^{-1}. The absorption intensity in the near-IR region (1000-1100 nm) is also very high. The broad absorption band from visible region to NIR region is the characteristics of the bipolaronic metallic state of doped polypyrrole. [23, 24, 38]

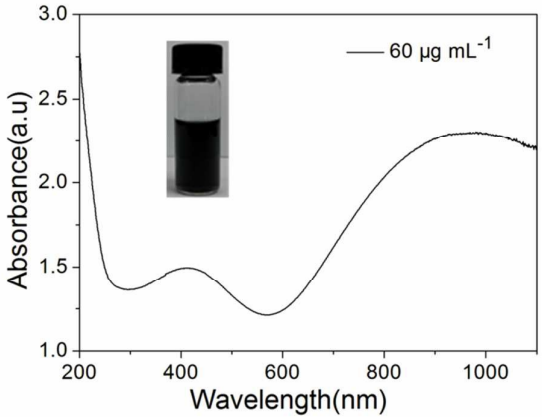

Fig. 4 UV-vis-NIR absorption spectrum of aqueous dispersion containing PPy nanoparticles (60 μg mL^{-1}). Inset: Photo of the aqueous dispersion.

As a result of their specific photoabsorption, PPy nanoparticles can absorb part of visible light while absorb strongly NIR light, probably resulting in the efficient photothermal conversion. To further investigate the photothermal performance, PPy nanoparticle powder (~0.5 mg) was directly put on the white paper (the inset in Fig. 5a). The temperature

distribution was recorded by thermal imaging camera under the irradiation of simulated solar light with the intensity of 0.5 W cm^{-2} (Fig. 5a). Before the light illumination, both PPy powder and the white paper remain the room temperature of 28.4 °C (Fig. 5b). When the solar light is turned on, the maximum temperature of PPy powder goes up rapidly with the increasing time to 30 s (Fig. 5a), and then exhibits a relatively slow increase to 70.5 °C at 180 s, as vividly shown in the thermographic image (Fig. 5c). The heating rate becomes slow with the increase of irradiated time, resulting from the faster heat loss at higher temperatures.[29, 32] Interestingly, white paper away from PPy sample remains low temperature of ~30.5 °C (Fig. 5c), although part of them was also irradiated simultaneously. Therefore, one can conclude that PPy nanoparticles can absorb solar light and convert efficiently it to heat.

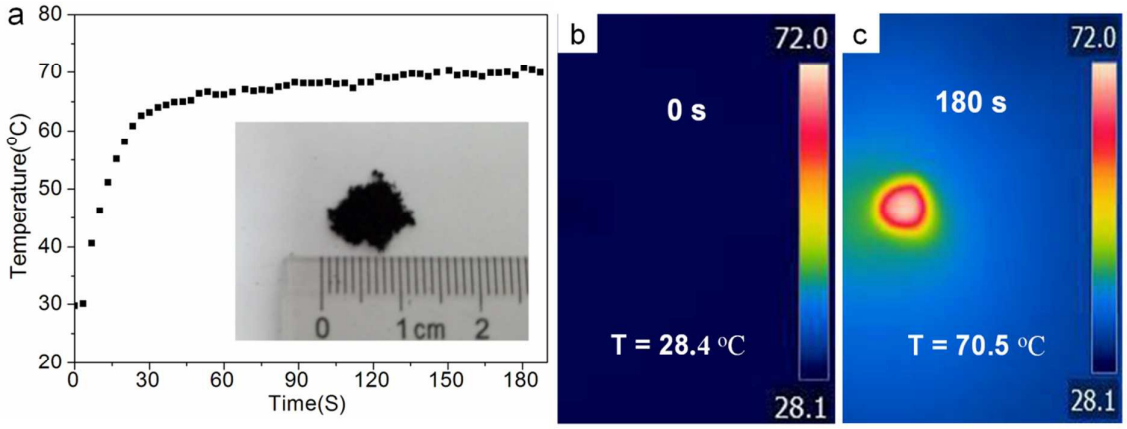

Fig. 5 (a) The temperature elevation of PPy powder on the white paper as a function of irradiation time with solar light (0.5 W cm^{-2}), the inset is the photo; (b,c) Thermographic images at 0 and 180 s irradiation.

3.2 Synthesis and NIR shielding property of PPy-PAA composite film

For satisfying visual effects but reducing the heating effect from solar light, it is important to develop UV/NIR shielding film which can transmit only visible light but cut off UV/NIR light. PPy nanoparticles exhibit good transparency in visible region and strong absorption in UV/NIR region, which motivates us to investigate their potential in UV/NIR

shielding films for buildings or automobile. In the present study, PPy nanoparticles were used as the photoabsorption agent, and PAA resin was used as the polymer matrix due to its advantages such as non-toxicity and optical transparence. PPy-PAA full polymer films were prepared by using coating-drying technology (Fig. 6a), where the slurries of PAA resin containing PPy nanoparticles were respectively coated on the glass slides, and then the slides were dried at 50 °C to solidify films (Fig. 6a). These films could be easily peeled off from the glass slides. Three PPy-PAA composite films with 0.05 wt% PPy and different thickness (about 0.34, 0.50, 0.60 mm) were prepared, and two 0.50-mm-thick films with different PPy content (0.10 wt% and 0.125 wt%) were also obtained.

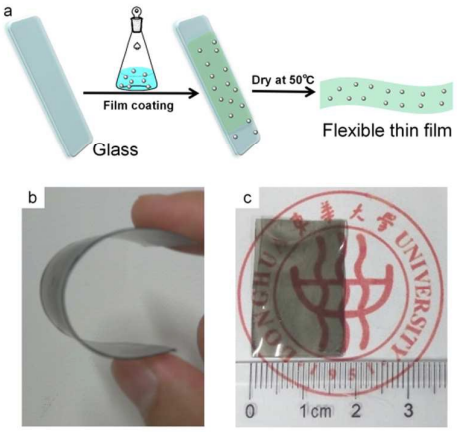

Fig. 6 (a) Schematic illustration of preparation process of the flexible PPy-PAA films. (b, c) Typical photographs of 0.34-mm-thick PPy-PAA film with 0.05 wt% PPy.

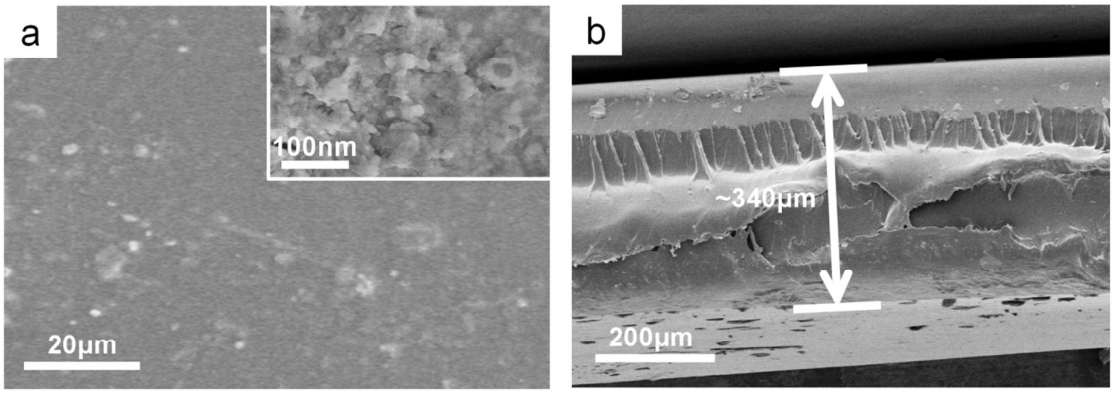

Fig. 7 Typical surface (a) and cross-section (b) morphologies of 0.34-mm-thick PPy-PAA film with 0.05 wt% PPy.

All these films have similar appearance, and they are light-black in color. Herein, 0.34-mm-thick PPy-PAA film with 0.05 wt% PPy was used as a model for the subsequent morphology analysis. It is clear that this film is free-standing and can be reversibly bent at large angles (0~360°) (Fig. 6b), resulting from the excellent flexibility of PAA matrix. Furthermore, this PPy-PAA film remains relatively transparent (Fig. 6c), which is favorable to keep good visual effects when being used as the window. Subsequently, we investigated the surface and cross-section morphologies by SEM images (Fig. 7). PPy-PAA film has very uniform and smooth surface without crack (Fig. 7a). From SEM image with higher magnification (the inset in Fig. 7a), one can find that there are many nanoparticles with good dispersibility in PAA film, suggesting that PPy nanoparticles was well encapsulated in PAA matrix. Undoubtedly, this encapsulation will avoid the direct contact between PPy nanoparticles and air/water, probably conferring the good weatherability of PPy-PAA film. In addition, the cross-sectional SEM image confirms that the thickness of this PPy-PAA film is ~0.34 mm (Fig. 7b), which agrees well with the data measured by vernier caliper.

The optical properties of these PPy-PAA films were studied by UV-visible-NIR spectrophotometer. Firstly, we investigated the effects of PPy content (0.05, 0.10, 0.125 wt%) on the transmittance of 0.50-mm-thick PPy-PAA films (Fig. 8a). For comparison, the transmittance spectrum of 0.5-mm-thick pure PAA film was also measured. Pure PAA film exhibits high transmittance (≥ 80%) in the entire UV-vis-NIR region (300-2500 nm), indicating the very low photoabsorption in the broad wavelength range. In addition, these three PPy-PAA films exhibit relatively high transmittance in visible region but low transmittance in UV and NIR region. With the increase of PPy content from 0.05 to 0.125 wt%, the entire transmittance goes down, where the maximum transmittance (T_{max}) at 579 nm

drops from 41.6% to 26.4%, and the average transmittance (T_{adv}) in 1100-2000 nm also decreases from ~15% to ~6%. In addition, we studied the change of the transmittance with film thickness by using PPy-PAA film with 0.05 wt% PPy and different thickness (0.34, 0.50, 0.60 mm) as the model (Fig. 8b). When the film thickness raises from 0.34 to 0.60 mm, the entire transmittance also declines, where T_{max} at 579 nm drops from 71.9% to 37.5% and T_{adv} in the wavelength of 1100-2000 nm goes down from ~18% to ~10%. All these results suggest that PPy-PAA films can transmit part of visible but absorb strongly NIR light. Undoubtedly, this visible transmittance and NIR shielding behavior of PPy-PAA films should be attributed to the presence of PPy nanoparticles, since PPy nanoparticles can absorb efficiently NIR light and then convert it to heat (Fig. 4,5) while PAA matrix has no obvious photoabsorption in a broad wavelength range (300-2500 nm). Furthermore, we also find that the visible transmittance and NIR shielding effects can be well controlled by adjusting PPy content and/or film thickness. For example, higher PPy content facilitates lower transmittance in NIR region, indicating higher NIR shielding effect.

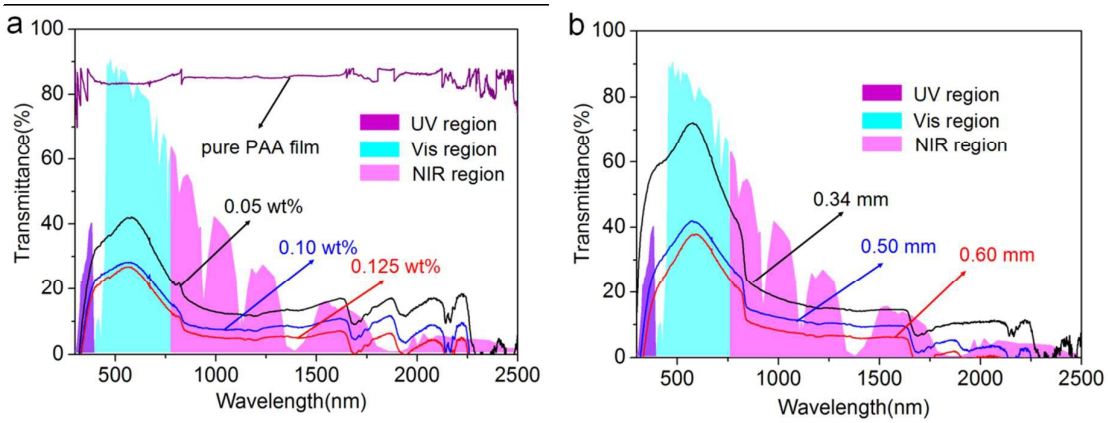

Fig. 8 Transmittance spectra of PPy-PAA films with (a) 0.50-mm-thickness with different PPy content (0, 0.05, 0.10, 0.125 wt%) and (b) 0.05 wt% PPy with different thickness (0.34, 0.50, 0.60 mm). For comparison, standard solar spectrum is also supplied.

Ideally, the photo-shielding film can only transmit visible light but cut off both NIR and

UV light. To determine the transmitted efficiency (**TE**) in visible region and shielding efficiency (**SE**) in NIR/UV region, we assume that PPy-PAA films are irradiated by a standard solar light (AM 1.5, 100 mW cm^{-2}), where the standard solar light spectrum are also shown in Fig. 8a,b. According to the transmittance spectra and standard solar spectrum (Fig. 8a,b), the transmitted intensity ($\boldsymbol{I}_T$) of different light (UV: 305-400 nm, VIS: 400-780 nm, NIR: 780-2500 nm) can be obtained by the equation (1):

$$I_T = \int F(\lambda)T(\lambda)\mathrm{d}\lambda \qquad (1)$$

where $F(\lambda)$ is the incident photon flux intensity at wavelength λ, and $T(\lambda)$ is the transmittance at wavelength λ. **TE** of different light can easily be obtained by the equation (2):

$$\mathbf{TE}=\frac{I_T}{I_{total}} \times 100\% \qquad (2)$$

where I_{total} is the total light intensity of different kind of solar light. **SE** of different light is the difference of 1 and its corresponding TE (such as, $\mathbf{SE_{NIR}}$= 1-$\mathbf{TE_{NIR}}$). The data of $\boldsymbol{I}_T$, **TE** and **SE** were summarized in Table 1.

Table 1 The data of transmitted intensity ($\boldsymbol{I}_T$), transmitted efficiency (**TE**), shielding efficiency (**SE**) and solar energy transmittance selectivity (SETS) for different (UV, Vis, NIR) light by different PPy-PAA films.

Type of PPy-PAA film	Transmitted Intensity (mW/cm^2)			Transmitted Efficiency (TE,%)			Shielding Efficiency (SE,%)			SETS
	UV	VIS	NIR	UV	VIS	NIR	UV	VIS	NIR	
0.50-mm+0.05 wt%	0.848	16.7	6.11	20.6	36.2	14.4	79.4	63.8	85.6	1.22
0.50-mm+0.10 wt%	0.561	11.4	3.52	13.6	24.7	8.28	86.4	75.3	91.7	1.16
0.50-mm+0.125 wt%	0.478	10.4	2.32	11.6	22.6	5.46	88.4	77.4	94.5	1.17
0.34-mm+0.05 wt%	2.16	29.1	8.08	52.8	63.1	19.1	47.2	36.9	80.9	1.44
0.60-mm+0.05 wt%	0.491	14.9	3.38	11.9	32.1	7.95	88.1	67.9	92.1	1.24

[a]The total light intensity from standard solar: UV (305-400nm)=4.11mW/cm^2, VIS (400-780 nm)=46.2 mW cm^{-2}, NIR (780-2500nm)=40.3 mW cm^{-2}.

For 0.50-mm thick PPy-PAA films with increasing PPy content from 0.05 wt% to 0.125 wt%, **TE** of visible light goes down from 36.2% to 22.6%, while **SE** of NIR light raises from

85.6% to 94.5%. Similarly, when the thickness of 0.05 wt% PPy film goes up from 0.34 to 0.60 mm, **TE** of visible light decreases from 63.1% to 32.1% while **SE** of NIR light increase from 80.9% to 92.1%. To evaluate the integrated optical performance of these PPy-PAA films, the solar energy transmittance selectivity (**SETS**) is denoted as the sum of **TE** of visible light and **SE** of NIR light. Since UV light has very low intensity in solar spectrum, herein we neglect its effect on **SETS**. **SETS** should have the range of 0-2, where 0 represents an opposite film that has no transmittance in visible region and no shielding ability in NIR region; and 2 represents an ideal film that can completely transmit visible but cut off all NIR light. According to Table 1, 0.34-mm-thick PPy-PAA film with 0.05 wt% PPy can transmit 63.1% visible light but block 80.9 % NIR light, yielding the highest **SETS** of 1.44. In fact, **SETS** can be tuned by adjusting PPy content and the film thickness (Table 1).

As a result of their moderate visible transmittance and high UV/NIR shielding, PPy-PAA films should have great potential as the semi-transparent heat-insulation coating of energy-saving windows for simultaneously satisfying visual effects and reducing the heating effect from solar light. To evaluate their heat-insulation performances, we constructed two sealed black boxes with glass slide or PPy-PAA film-coated glass (2×6 cm^2) as the window (Fig. 1). Under the irradiation of the simulated solar light with high intensity (0.3 or 0.5 W cm^{-2}), the air-temperature in the box was real-time recorded, as shown in Fig. 9. Obviously, the interior air temperature goes up rapidly with irradiated time to 300 s, and then exhibits a relative flat and reaches a maximum at 1500 s. The maximum temperature elevation (ΔT) is determined to investigate the heat-insulation performance of the window. When the solar light intensity is 0.3 W cm^{-2}, the ordinal glass slide as the blank window confers a temperature elevation (ΔT_l=7.3 °C) (Fig. 9a). For two typical PPy-PAA films (0.34-mm-thick+0.05wt%

PPy; 0.50-mm-thick+0.125 wt% PPy) coated glass as the test window, the temperature elevation is respectively 4.2 and 3.5 °C (Fig. 9a), which is just about 57.5% and 48.6% of that (ΔT_1=7.3 °C) from glass slide. Similarly, under the illumination of solar light with higher intensity (0.5 Wcm^{-2}), the temperature elevation from PPy-PAA films (0.34-mm-thick+0.05wt% PPy; 0.50-mm-thick+0.125 wt% PPy) coated glass is 8.9 and 7.1 °C (Fig. 9b), which is just 56.7% and 45.2 % of that (ΔT_4=15.7 °C) from glass slide. These facts reveal that the temperature elevation from PPy-PAA films coated glass is much lower than that from glass slide, with a large difference.

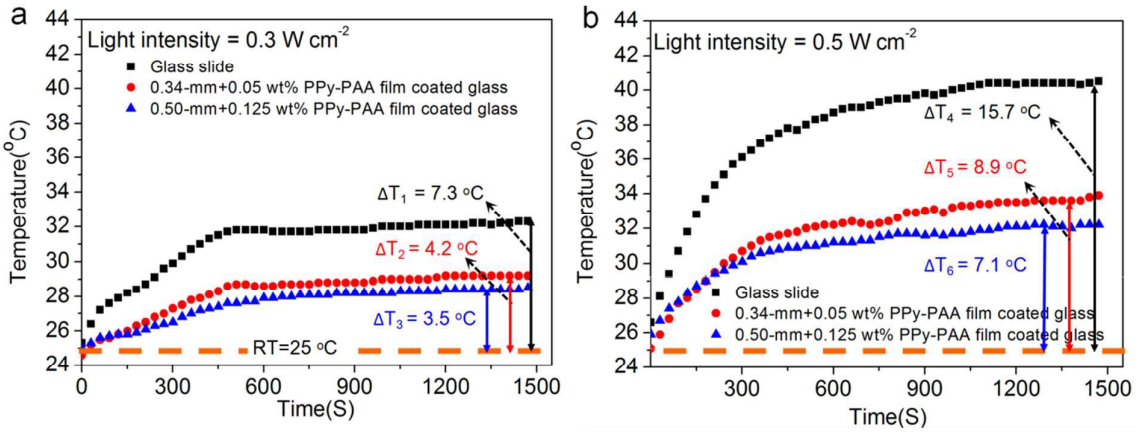

Fig. 9 The changes of the interior air temperature of the box with the glass slide or PPy-PAA film (0.34-mm-thick+0.05wt% PPy; or 0.50-mm-thick+0.125 wt% PPy) coated glass as the window, as a function of time under the irradiation of solar light with intensity of (a) 0.3 and (b) 0.5 W cm^{-2}.

It is well known that the glass slide has very high transparency in the almost entire solar spectrum (300-2500 nm). Thus, almost all solar light can transmit glass slide window and reach the interior of the box, resulting in strong heating effect and then large temperature elevation. Usually, the large temperature elevation easily makes human uncomfortable and then increases the energy consumption of buildings or vehicles. Importantly, the introduction of PPy-PAA films results in low temperature elevation, since PPy-PAA film can shield part of

visible light and almost all NIR light, as shown in (Fig. 8, Table 1). In addition, although PPy-PAA films are used as the coating, the interior air temperature will also go up inevitably, since visible light should be transmitted for satisfying visual effects. But we can expect that the temperature elevation can be well tuned by changing photo shielding effect, for example, by adjusting PPy content and the film thickness or using the combination of different films. More importantly, the present PPy-PAA film has low-cost and is metal-free; and the abandon of the films will not result in heavy-metal pollution, both of which will be favorable for the design and development of cost-efficient energy-saving windows without potential pollution.

4. Conclusions

PPy nanoparticles with size of ~50 nm have been synthesized by a modified one-step aqueous dispersion polymerization method, and they can transmit par of visible light and absorb efficiently UV/NIR light. With PPy nanoparticles as the photoabsorbing agent, PPy-PAA full-polymer films have been prepared and remain the moderate visible transmittance and efficient NIR shielding. Importantly, when PPy-PAA film coated glass is used as the window of the sealed box, the interior air temperature exhibits low elevation (3.5~8.9 °C) compared with (7.3~15.7 °C) from glass slide as window, under the irradiation of the simulated solar light with high intensity (0.3, 0.5 W cm^{-2}). Therefore, PPy-PAA full polymer films have great potential as novel coating in the application of cost-efficient energy-saving windows without potential pollution

Acknowledgements

This work was financially supported by the National Natural Science Foundation of

China (Grant No. 21477019, 51272299, and 51473033), Program for Changjiang Scholars and Innovative Research Team in University (Grant No. IRT1221 and T2011079), project of the Shanghai Committee of Science and Technology (13JC1400300). Innovation Program of Shanghai Municipal Education Commission (Grant No. 13ZZ053), Shanghai Leading Academic Discipline Project (Grant No. B603), the Fundamental Research Funds for the Central Universities, and DHU Distinguished Young Professor Program.

Notes and references

1. R. Pardo, M. Zayat and D. Levy, *Chem. Soc. Rev.*, 2011, **40**, 672-687.
2. A. Seeboth, D. Lötzsch, R. Ruhmann and O. Muehling, *Chem. Rev.*, 2014, **114**, 3037-3068.
3. R.-T. Wen, C. G. Granqvist and G. A. Niklasson, *Adv. Funct. Mater.*, 2015, **25**, 3359-3370.
4. J. Kim, G. K. Ong, Y. Wang, G. LeBlanc, T. E. Williams, T. M. Mattox, B. A. Helms and D. J. Milliron, *Nano Lett.*, 2015, **15**, 5574-5579.
5. S. Cong, Y. Tian, Q. Li, Z. Zhao and F. Geng, *Adv. Mater.*, 2014, **26**, 4260-4267.
6. J. Yao, K. Hashimoto and A. Fujishima, *Nature*, 1992, **355**, 624-626.
7. B. Fang, Y. Li, G. Tong, X. Wang, M. Yan, Q. Liang, F. Wang, Y. Qin, J. Ding and S. Chen, *Opt. Mater.*, 2015, **47**, 225-230.
8. D. Miao, S. Jiang, S. Shang and Z. Chen, *Vacuum*, 2014, **106**, 1-4.
9. D. Miao, S. Jiang, S. Shang, H. Zhao and Z. Chen, *J. Mater. Sci.: Mater. El.*, 2014, **25**, 5248-5254.
10. C. L. Tan, S. J. Jang and Y. T. Lee, *Opt. Express*, 2012, **20**, 17448-17455.

11. T. T. Xu, J.-G. Zheng, A. W. Nicholls, S. Stankovich, R. D. Piner and R. S. Ruoff, *Nano Lett.*, 2004, **4**, 2051-2055.
12. K. Adachi, M. Miratsu and T. Asahi, *J. Mater. Res.*, 2010, **25**, 510-521.
13. M. Kanehara, H. Koike, T. Yoshinaga and T. Teranishi, *J. Am. Chem. Soc.*, 2009, **131**, 17736-17737.
14. A. Llordés, G. Garcia, J. Gazquez and D. J. Milliron, *Nature*, 2013, **500**, 323-326.
15. D. Miao, S. Jiang, S. Shang, Z. Chen and J. Liu, *Adv. Perform. Mater.*, 2014, **29**, 321-325.
16. Q. Tan, G. Yu, Y. Liao, B. Hu and X. Zhang, *Colloid Polym. Sci.*, 2014, **292**, 3233-3241.
17. C. Guo, S. Yin, Y. Huang, Q. Dong and T. Sato, *Langmuir.*, 2011, **27**, 12172-12178.
18. C. Guo, S. Yin, M. Yan, M. Kobayashi, M. Kakihana and T. Sato, *Inorg. Chem.*, 2012, **51**, 4763-4771.
19. C. Guo, S. Yin, Q. Dong and T. Sato, *CrystEngComm*, 2012, **14**, 7727-7732.
20. C. Guo, S. Yin, L. Huang and T. Sato, *ACS Appl. Mater. Inter.*, 2011, **3**, 2794-2799.
21. C. Guo, S. Yin, L. Huang, L. Yang and T. Sato, *Chem. Commun.*, 2011, **47**, 8853-8855.
22. X. Zeng, Y. Zhou, S. Ji, H. Luo, H. Yao, X. Huang and P. Jin, *J. Mater. Chem. C*, 2015, **3**, 8050-8060.
23. K. Yang, H. Xu, L. Cheng, C. Sun, J. Wang and Z. Liu, *Adv. Mater.*, 2012, **24**, 5586-5592.
24. Z. Zha, X. Yue, Q. Ren and Z. Dai, *Adv. Mater.*, 2013, **25**, 777-782.
25. H. Deng, F. Y. Dai, G. H. Ma and X. Zhang, *Adv. Mater.*, 2015, **27**, 3645-3653.
26. M. S. Yavuz, Y. Cheng, J. Chen, C. M. Cobley, Q. Zhang, M. Rycenga, J. Xie, C. Kim, K. H. Song and A. G. Schwartz, *Nat. Mater.*, 2009, **8**, 935-939.
27. K. Yang, L. Feng, X. Shi and Z. Liu, *Chem. Soc. Rev.*, 2013, **42**, 530-547.
28. Y. Li, W. Lu, Q. Huang, C. Li and W. Chen, *Nanomedicine*, 2010, **5**, 1161-1171.

29. Z. Chen, Q. Wang, H. Wang, L. Zhang, G. Song, L. Song, J. Hu, H. Wang, J. Liu and M. Zhu, *Adv. Mater.*, 2013, **25**, 2095-2100.
30. W. Xu, Q. Tian, Z. Chen, M. Xia, D. K. Macharia, B. Sun, L. Tian, Y. Wang and M. Zhu, *J. Mater. Chem. B*, 2014, **2**, 5594-5601.
31. W. Xu, Z. Meng, N. Yu, Z. Chen, B. Sun, X. Jiang and M. Zhu, *RSC Adv.*, 2015, **5**, 7074-7082.
32. Q. Tian, M. Tang, Y. Sun, R. Zou, Z. Chen, M. Zhu, S. Yang, J. Wang, J. Wang and J. Hu, *Adv. Mater.*, 2011, **23**, 3542-3547.
33. Q. Tian, F. Jiang, R. Zou, Q. Liu, Z. Chen, M. Zhu, S. Yang, J. Wang, J. Wang and J. Hu, *ACS nano*, 2011, **5**, 9761-9771.
34. Q. Tian, J. Hu, Y. Zhu, R. Zou, Z. Chen, S. Yang, R. Li, Q. Su, Y. Han and X. Liu, *J. Am. Chem. Soc.*, 2013, **135**, 8571-8577.
35. M. Omastová, M. Trchová, J. Kovářová and J. Stejskal, *Synthetic. Met.*, 2003, **138**, 447-455.
36. H. de Oliveira, C. Andrade and C. de Melo, *J. Colloid Interf. Sci*, 2008, **319**, 441-449.
37. R. Kostić, D. Raković, S. A. Stepanyan, I. E. Davidova and L. A. Gribov, *J. Chem. Phys.*, 1995, **102**, 3104.
38. R. B. Bjorklund and B. Liedberg, *Chem. Commun.*, 1986, 1293-1295.

Graphical Abstract

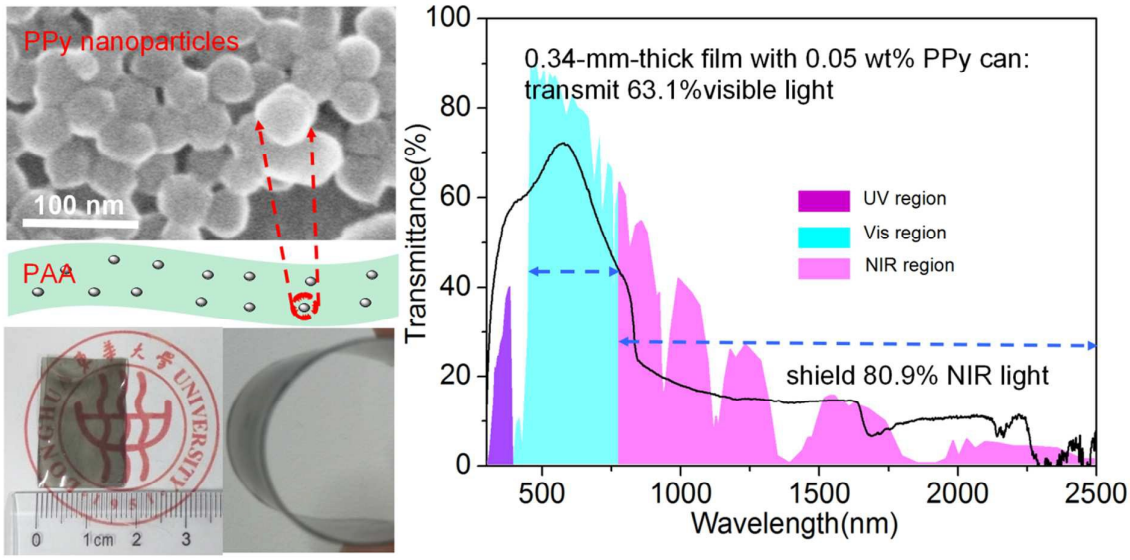

Polypyrrole (PPy) nanoparticles with diameter of ~50 nm were synthesized, and the corresponding flexible PPy-polyacrylic acid (PAA) full-polymer films can transmit visible light but efficiently block UV/NIR light.